Experimental trials and theoretical background about foaming, slag refractory interaction and feasibility of crude magnesium carbonate injection as foaming agent and its use for EAF refractory protection

C. Mapelli, D. Mombelli, S. Barella, P. Trezzi, G. Ferrari, C. Cagni

A theoretical overview about the slag structure, their compatibility with the refractories and their foaming behavior has been realized. Such a theoretical background is the basis for the performed experimental trials focused on the use of crude $MgCO_3$ injected within the slag. This raw material can develop the gaseous phases (CO_2) needed for the slag foaming and it can provide the MgO useful to make the slag compatible with the refractories. The experimentation has been performed through the injection of different specific quantities of $MgCO_3$ and the obtained results pointed out a significant decrease of refractory wear, a saving of the specific electric energy, a decrease of the lime injection and of the anthracite powder needed to induce the foaming effect.

Keywords: Slag - Refractory - Foaming - Crude Magnesite Injection

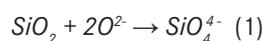## THEORETICAL BACKGROUND ABOUT THE SLAG BEHAVIOR

The electric arc furnace slags are complex solutions of variable compositions formed during the oxidizing refining processes and the deoxidation period inside the electric arc furnace (EAF). The slag is formed over the molten steel as a result of the oxidation of ferrous scraps and of the compounds generated by the additives included in the charge of the electric furnace. Thus, their chemical compositions depend upon the quality of the scraps used for the steel production and, to a lesser extent,

Carlo Mapelli, Davide Mombelli, Silvia Barella

*Dipartimento di Meccanica, Politecnico di Milano,
Via La Masa, 1 - 20156 Milano (ITALY)*

Pietro Trezzi, Guido Ferrari

*Trezzi Refrattari S.r.l.
Via Alberico da Merlino, 5 - 26833 Merlino (LO) (ITALY)*

Claudio Cagni

*Duferdofin Nucor S.r.l.,
Via Armando Diaz, 248 - 25010 San Zeno Naviglio (BS) (ITALY)*

Corresponding author

*Davide Mombelli: davide.mombelli@mail.polimi.it
Pietro Trezzi: pietro@trezzirefrattari.com
Guido Ferrari: ferrari1410@ferrari1410.it*

on the refractory linings quality. Actually, the chemical composition of the refractory must be compatible with that of the slag to prevent excessive and rapid dissolution of the furnace linings coating.
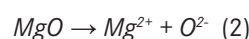
The EAF slags at the molten state are ionic solutions characterized by the presence of cations (positive charges: Ca^{2+}, Ba^{2+}, etch.) and anions (negative charges: O^{2-}, S^-). On the contrary, outside the furnace, after cooling, the solidified slags are ionic or covalent and ionic materials. The covalent-polar contribution is determined by the presence of tetrahedral elementary structures, i.e. SiO_4^{4-}; AlO^{4-}, characterized by strong covalent bonds between the metallic cations (Si, Al) and the oxygen anions. The ionic nature, instead, is determined by the difference in electronegativity between cations (Ca^{2+}) and anions (SiO_4^{4-}).

The steel slags are formed primarily from oxides and to a lesser extent by sulfides and phosphates. The chemical species present in the slag can be classified into two principal categories:

- glass promoter chemical species (also called acidic species): SiO_2, P_2O_5. They absorb anions (equation 1);

$$SiO_2 + 2O^{2-} \rightarrow SiO_4^{4-} \quad (1)$$

- glass modifier chemical species (also called basic species): FeO, MgO, CaO, BaO e Na_2O. They form cations (equation 2).

$$MgO \rightarrow Mg^{2+} + O^{2-} \quad (2)$$

Glass promoter species tend to polymerize and to form lattice structures. The most important glass promoter is silica (SiO_2), which tends to reticulate forming oxygen bridges that link the silicon cations. In the three-dimensional space the silicon appears in the center of a tetrahedron whose vertices are occupied by oxygen atoms: this is the fundamental structure of silicates (SiO_4^{4-}). In the case of phosphate, the basic structure will consist in PO_4^{3-}. The glass modifiers (basic species), instead of forming cross-linked structures thanks to the presence of oxygen bridges, are donor of oxygen atoms, therefore tend to yield the oxygen atoms, creating an effect of disruption on the reticular structure. There are three principal actions of network modifiers in glasses, which can be summarized for a generic A_2O_3 glass as follows:

• breaking of A–O–A bonds and creation of non-bridging oxygens;
• increasing the oxygen coordination of cation A;
• a combination of both.

There are also the so-called amphoteric species, which tend to behave as donor of oxygen when they are associated with acidic species or act as glass promoter when in the presence of chemical species with basic features. The usual amphoteric species in the steel slag are Al_2O_3, Fe_2O_3, B_2O_3 and MnO. For example, when Al_2O_3 is associated with basic chemical species it tends to form reticular structures whose fundamental structure is constituted by AlO_3^{3-}.

The slag fulfills important metallurgical tasks, such as regulating the oxygen potential at the slag-metal interface, determine the EAF process progression and allow the desulphurization and dephosphorization. To function optimally, the slag must be liquid (at process temperatures inside the furnace) and possess a proper fluidity to control the foaming. Slag can have significant viscosity due to the important fraction of cross-linking oxides, that is usually reduced by the introduction of glass modifiers, which hinder the cross-linking process. Actually, the basic slags are characterized by particularly high melting points and thus, acidic and basic species mix leads to the formation of basic slag characterized by low-melting temperature eutectic phases.

The relationship between the concentrations of acidic species and basic species (basicity index) allows to express and interpret important slag-metal equilibriums, such as the oxidizing power of the slag, the desulphurization and dephosphorization equilibriums, and the slag-metal breakdown. Basicity coefficient defines the slag basicity, weighting the content of acidic and basic species. The simplest index is B2, defined as ratio between CaO and SiO_2 fraction in the slag. A more complex index can be defined including in the count the other chemical species, i.e. B5 index (equation 3). Typically a slag is defined acidic for basicity coefficients lower than 1.

$$B5 = \frac{\%CaO + \%MgO}{\%SiO_2 + \%Al_2O_3 + \%FeO_x} \quad (3)$$

The use of the basicity coefficients does not account for the different capacity of reticulating or donating oxygen featuring the different chemical species involved.

To compensate this lack, the concept of optical basicity was introduced [1]. Optical basicity (Λ) is a basicity indicator of the slag and it has been formulated by Duffy and Ingram, using spectrographic information coupled with the electronegativity data defined by Pauling. The optical basicity for a slag could be computed according to equation (4),

$$\Lambda = \sum_i x_i \cdot \Lambda_i \quad (4)$$

where Λ is the calculated optical basicity; Λ_i is the specific optical basicity of i-oxide species listed by Duffy and Ingramm and revised by Leboutellier and Cournten [2]; X_i is the weighed average content of i-oxide species, calculated by equation (5), where N_c is the molar fraction of oxide species and n_{Ox-C} is the number of oxygen constituting the oxide.

$$x_i = \frac{\Lambda = N_c \cdot n_{Ox-C}}{\sum_c N_c \cdot n_{Ox-C}} \quad (5)$$

The optical basicity has proved to be an extremely important parameter for characterizing the interaction between the slag and the metal bath. For example, Duffy and Ingram defined the S-bearing power of the slag as a function of its optical basicity. Thus, it is possible to estimate the maximum S content could be seized in the slag, providing real-time composition corrections to have the best desulfurization of the bath [1].

During the production process, the slag is made up of only liquid or liquid and solid fraction; the latter consists predominantly of calcium silicates ($2CaO \cdot SiO_2$ and, to a lesser extent of $3CaO \cdot SiO_2$) and $CaO \cdot Fe_2O_3$, whereas the liquid fraction is composed mainly of magnesium-wustite (FeO-MgO). Specifically for the EAF process, the solid fraction is crucial to control the viscosity and thus the foaming of the slag, which depends on the ability of the latter to trap the CO bubbles. During the melting period, both electric arc and oxygen flux are active: thanks to the injection of pulverized coke, CO bubbles could develop inside the slag, allowing its foaming. An intense foaming takes place after the preferential oxidation of silicon and manganese, when oxygen is consumed by the carbon contained in the droplets of molten metal dispersed in the slag saturated by FeO. The foam formation in this period becomes more intense because the volume of the gaseous phase constituted by the bubbles doubles. The added CaO and/or MgO contribute to control the slag viscosity, acting on the solid fraction of the slag, thus regulating the foaming process. In fact, the solid fraction depends on the concentration of the basic oxides present and on the amount of iron oxides: the increase in MgO and CaO and the decrease in iron oxides, increase the solid fraction. To adjust the slag chemical composition in order to have enough solid fraction to control the foaming, specific diagrams could be used [3]. Those phase diagrams asses the presence of the solid fraction and the compounds present in it as a function of
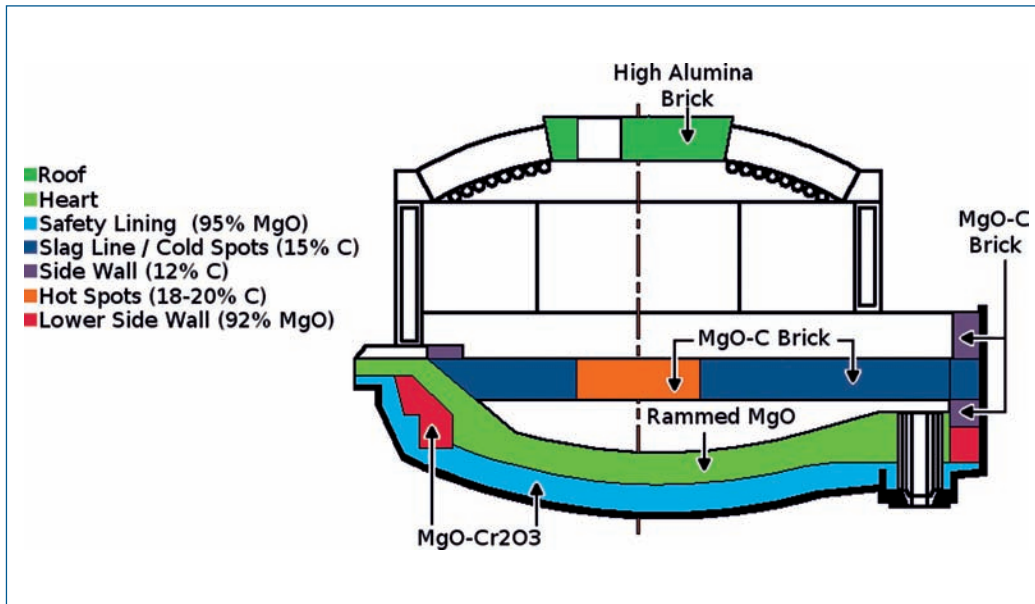
Fig. 1 - Schematic cross section of an electric arc furnace indicating the typical refractories employed.

Fig. 1 - Schema di una sezione del forno elettrico ad arco e dei refrattari tipicamente utilizzati per le diverse zone.

the concentration of MgO and FeO, for a specific basicity. Increasing the temperature, the area of existence of the liquid phase increases, too. Above the 35% by weight of iron oxides, a solid fraction, enough to maintain the emulsion stable and then the foam, becomes complicated to be maintained.

Many advantages can be achieved working with foaming slag:

• higher productivity, with short tap-to-tap time, due to the higher temperature and the best heat transfer from the arc to the bath;

• lower electrodes specific consumption, due to the lower current intensity, and shorter operating times and lower oxidation;

• lower thermal stresses of the refractory lining, because the arc is almost submerged by the slag, which is interposed as a screen between the refractory and the arc absorbing the radiant energy;

• less noisy arc;

• lower nitrogen uptake in the metal bath.

Generally, the EAF slag should be saturated in MgO, to be in equilibrium with the refractory lining; otherwise the latter would be dissolved through a chemical attack, which leads to a rapid consumption of the refractory in contact with the slag. Being lime and magnesia two compounds with basic characteristics, the solubility of MgO decreases with the increasing the CaO concentration.

The classification based on the basicity index can be extended also to the refractory materials used to protect the inner side of the electric arc furnace. Specifically, refractories can be distinguished as acidic, basic or neutral as a function of their chemical composition [4,5].

Acidic refractories tend to react with basic slag. The most common are the silico-aluminous clay refractories, made of by silica and 20-44% by weight of Al_2O_3. Those with more than 50% by weight of Al_2O_3 are defined aluminous whereas the mullite-base refractories have over the 60% of Al_2O_3. Finally, if the concentration of Al_2O_3 is higher than the 95%

by weight, the refractory is defined as corundum.

The basic refractories react with acidic slag and consist mainly in magnesia (MgO) or lime (CaO). Largely employed is also the dolomite, produced by sintering after decarbonation of dolomia (30.4% CaO, 21.9% MgO e 47.7% CO_2) and featured by very small amount of SiO_2 (less than 2%) [4,6,7].

The neutral refractories are mostly based on graphite and chromite ($FeCr_2O_4$). They are characterized by high chemical inertness and good resistance to contact both with acidic and basic slag.

The inner side of the EAF chamber is coated by refractory bricks, usually made of cooked magnesite or low carbon tempered magnesite, but in the hot spots, high thermochemical stability being required, MgO-C bricks are employed (Figure 1). The quality and the characteristics of refractory bricks are related to the areas they cover: critical zones, like slag line or hot spots, require high mechanical strength bricks featured by high chemical stability, low porosity and good conductivity. Indeed, during the melting operation, the exposure to the thermal action of the arc, the contact with the slag and the liquid steel, the movement of the bath and the impact of scrap can determine a progressive wear in the refractory lining.

The refractory wear consists in a loss of thickness and mass from the exposed face of the refractory as a consequence of chemical attack by the slag in a process in which the refractory and the slag react, approaching chemical equilibrium in the contact zone.

Corrosion reactions should be viewed as attempts of the system to achieve compatibility by progressing toward equilibrium. Refractories are rarely at chemical equilibrium on a microscopic scale, since they are typically made of mixtures of different minerals. However, at the immediate corrosion interface between the refractory and the slag, the localized volume elements may be at or close to chemical equilibrium.

The refractory has a temperature gradient from the hot
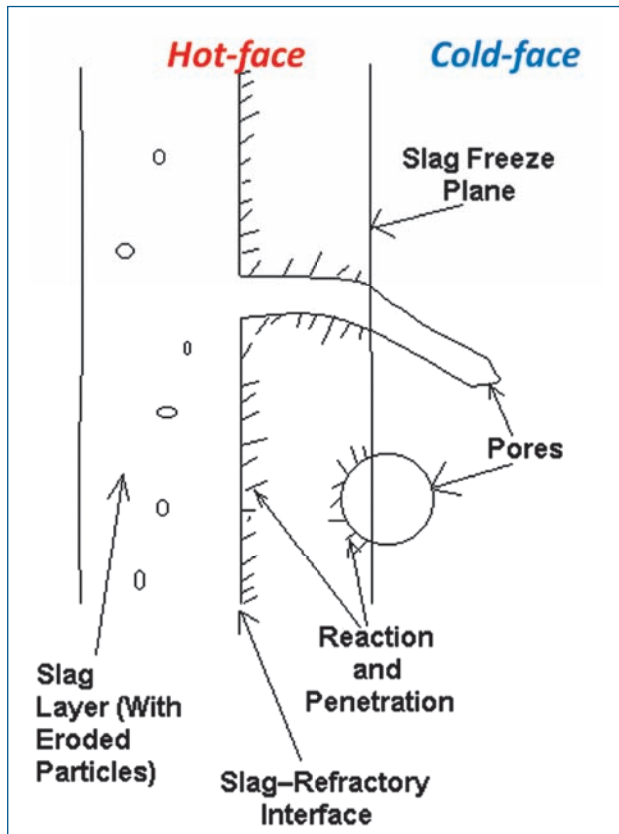
Fig. 2 - Cross section of the slag-refractory interfacial area [8].

Fig. 2 - Sezione trasversale dell'area di interfaccia tra scoria e refrattario [8].

to the cold-face, meaning that the highest temperature is at the hot-face and the temperature declines across the refractory thickness toward its back or cold side. Slag usually penetrates the refractory until the "freeze plane" is reached, that is the location in the refractory where the temperature is sufficiently low to cause the slag to solidify (Figure 2).

Slag reacts with the refractory, forming new phases at the immediate hot-face. Reaction also takes place behind the hot-face, where slag contacts the refractory at the pore walls. The temperature gradient affects the extent of phenomena seen in slag corrosion. In conventional refractory designs, the lining is at least one brick thickness (> 225 mm), and the lining typically features a safety lining for a total thickness of at least 450 mm. The slag freeze plane may be located in a zone of 40-75 mm behind the hot-face, even if, in some cases, slag may penetrate up to 150 mm behind the hot-face. The refractory corrosion reactions occur primarily at the immediate hot-face, and there is little or no slag penetration. Usually, penetration is confined to a depth of less than 100 µm behind the exposed hot-face. This situation is called "Stage I" (Figure 3a).

The hot-face temperature primarily affects the rate of corrosion reactions. Actually, if the hot-face temperature is held just below the point when the products of cor-

rosion become liquid (melt), corrosion will be very slow or nonexistent. If the hot-face is maintained at no more than 20 °C above the lowest eutectic temperature, reasonable corrosion rates will be observed. However, when the hot-face temperature is more than 20 °C above the eutectic, corrosion is rapid. Thin-wall refractory designs rarely exhibit more extensive corrosion phenomena that are described as "Stage I". Therefore, the primary process variable affecting corrosion is the hot-face temperature. Secondary variables influencing corrosion rates include slag impingement velocity and slag chemistry. With respect to chemistry, the refractory will be soluble in the slag up to a certain extent (or percentage). If the slag is "satisfied" with respect to the refractory chemistry, slag corrosion should be minimal. The term "satisfied" means that the slag has reached the chemical solubility limit of major refractory constituents in the slag.

Because of the broad temperature gradient, the refractory is penetrated by slag. Penetration is aided by capillary suction, as the smallest pores in the refractory (diameter 10 µm) draw the liquid slag behind the hot-face. In time, extensive corrosion of the refractory takes place. This situation is called "Stage II" (Figure 3b) and is characterized by two phenomena: (1) full penetration of the refractory and (2) extensive disruption by corrosion of the hot-face region. Stage II follows Stage I only if there is a sufficiently broad temperature gradient to allow penetration. In Stage II, the coarse aggregate in a bonded refractory exhibits penetration, particularly along grain boundaries (boundaries between crystals making up polycrystalline aggregate particles). The direct bonding between the matrix and the aggregate particles is disrupted, but this bonding still exists. Slag penetration in Stage II can result in densification spalling, that occurs because the thermal expansion coefficient in the slag penetrated zone is different than that in the unpenetrated cold-face region. On continued thermal excursions (cooling and heating), spalling can occur at the line of demarcation between penetrated and unpenetrated areas. The residual lining, after spalling, then begins the corrosion process anew, progressing from Stage I to Stage II again.

Toward the end of the refractory lining's life, or in cases of relatively slow corrosion rates and where densification spalling has not taken place, the refractory hot-face zone may progress to a final stage of corrosion that may be called "Stage III" (Figure 3c). In this case, bonding in the hot-face region and up to 2 to 4 mm behind the hot-face is minimal. The slag itself appears to be the only phase holding the residual aggregate particles in place. This is probably a result of the higher viscosity of the slag in the hot-face region created as a consequence of dissolution of the refractory in the slag.

Beside the corrosive attack induced by the slag on the refractory lining, a mechanical wear takes also place at the slag-refractory interface. The motion of the slag film caused by surface tension phenomena (wettability) between the refractory and the slag essentially causes the local corrosion of refractories at the slag surface (Fi-
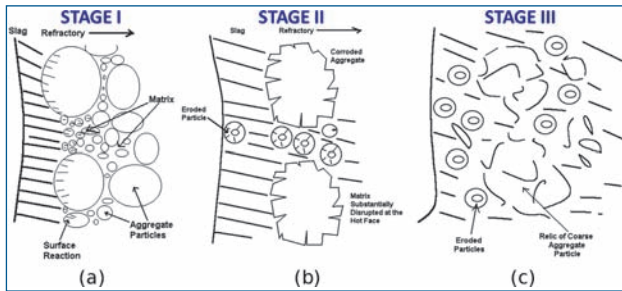
Fig. 3 - Different stages featuring a process of refractory wear by chemical interaction with the slag [8].

Fig. 3 - Differenti stadi di un processo di usura del refrattario, dovuta all'interazione chimica con la scoria [8]

gure 4). This is because the slag film motion accelerates the dissolution rate of the refractory and also induces the abrasion of some refractories [9]. The active film motion is dominantly induced by the Marangoni effect [10,11] and/or change in the form of the slag film due to the variation of the surface tension and the density of the slag film. The local corrosion of refractories at the slag/metal interface is also explained reasonably by a mechanism, which is similar to that of the refractory/slag system.
Thus, the chemical corrosion and the mechanical interaction represent the two main processes affecting the soundness and the life of the refractories.

THEORETICAL BACKGROUND ABOUT FOAMING

The slag foaming represents an operative practice applied during the dephosphorization and the decarburation steps. Such an operative practice is applied for avoiding the direct exposition of the refractories to the radiation of the electric arc and for improving the heat transfer from the arc to the steel bath. The main chemical reaction ruling the foaming slag is associated to the formation of the carbon monoxide, produced by the reduction of the iron oxide droplets developed by the oxygen injection (Figure 5). Such a sequence of chemical reaction is described by the relation (6) and (7):

$$2Fe + O_2 \rightarrow 2FeO \qquad (6)$$

$$FeO + C \rightarrow CO_{(gas)} + Fe \qquad (7)$$
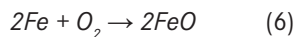
This combination of reactions is endothermic and is featured by a heat absorption of +158 kJ/mol. Thus, the foaming reaction performed by the reduction of iron oxide implies a cooling of the slag system. Actually, an excess in the graphite powder addition can cause the detrimental consequence of an increase in the electric energy supply, provided a constant supply of methane (Figure 6).
On the other hand, other chemical reactions can be exploited in order to allow the development of gas phases within the slag:

$$CaCO_3 \rightarrow CaO + CO_2 \qquad (8)$$

$$MgCO_3 \rightarrow MgO + CO_2 \qquad (9)$$
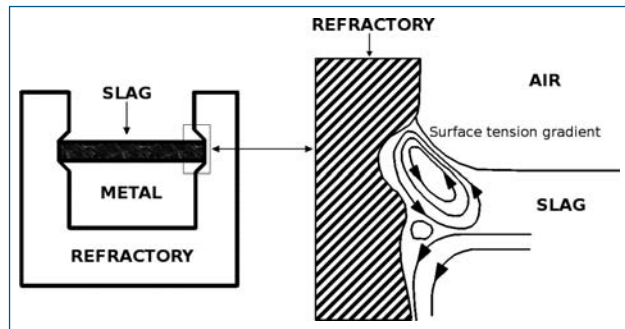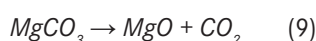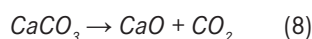
Fig. 4 - Mechanical interaction between the slag and the surrounding refractory lining due to the effect of the surface tension [9].

Fig. 4 - Interazione meccanica tra la scoria ed il rivestimento refrattario, dovuta all'effetto della tensione superficiale [9].
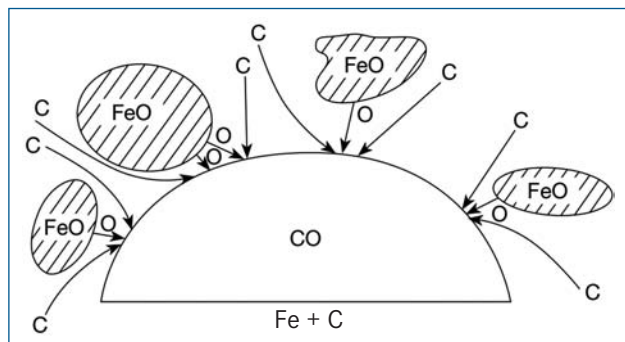
Fig. 5 - Scheme of CO bubble formation in slag through the reaction among iron oxide droplets, carbon and oxygen [12].

Fig. 5 - Schema della formazione di bolle di CO all'interno della scoria dovuta all'interazione tra gocce di ossido di ferro, carbonio ed ossigeno insufflato [12].
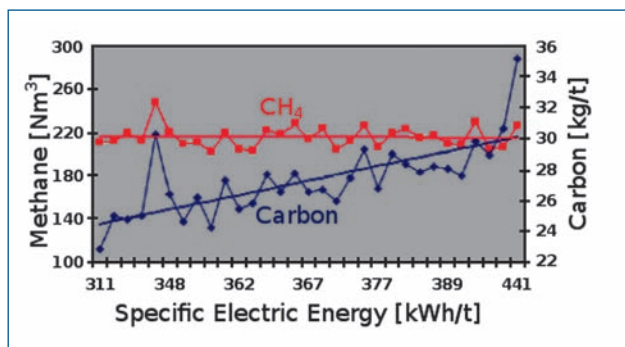
Fig. 6 - Experimental measurements showing the increase of the supplied specific electric energy as the specific carbon supply increases and the overall specific injected methane volume is maintained constant.

Fig. 6 - Misure sperimentali riguardanti l'incremento di energia elettrica specifica in funzione dell'incremento della quantità di polverino di carbone (in genere costituito da antracite) a parità di volume di metano iniettato.

At the pressure of 1 atm the reaction (8) takes place at 840 °C and it is associated to a heat absorption of +178 kJ/mol, whereas the reaction (9) occurs at 662 °C with a heat absorption of +118 kJ/mol. Thus, the reactions (8) and (9) can provide the gaseous phases for the slag foaming involving lower heat absorption. Moreover, such reactions can provide CaO and MgO within the slag, so if the saturation is reached such chemical species can make the slag inert for the refractories linings. The CaO is added to the slag to perform the phosphorus removal from the steel bath; thus, the slag is certainly saturated by this chemical species or by chemical species featured by a high CaO activity ($2CaO \cdot SiO_2$). On the contrary, MgO is specifically added to reach the saturation concentration needed to preserve the MgO content of the dolomite or MgO-based refractory. Thus, the addition of $MgCO_3$ can be exploited as a foaming agent and for MgO enrichment of the slag in order to make slag itself inert for the EAF refractories. The addition of $MgCO_3$ seems to represent an interesting option as a foaming agent and for the refractory protection because it is even featured by lower energy absorption.
The precipitation of solid fine particles increases the viscosity of the slag, that can be described through the Einstein-Roscoe relation (equation 10):

$$\eta = \frac{\eta_0}{(1-\alpha f)^n} \qquad (10)$$

where:

η is the liquid slag viscosity modified by the presence of dispersed solid particles;
η_0 is the liquid slag viscosity;
f is the fraction of solid particles;
α is a characteristic constant assuming a value of 1.35;
n is a characteristic constant assuming a value of 2.5.

As the viscosity increases, the stability of the slag foam increases too, because the liquid drainage between the foam bubbles is ruled by the liquid slag viscosity and by the area of the Plateau borders, among which the liquid slag is drained by the gravity force [13] (equation 11):

$$\dot{X} = \frac{g\rho A_{plateau}}{\eta} \left[1 - exp\left(- \frac{\eta}{\rho A_{plateau}} t\right) \right] \qquad (11)$$

where:

$\dot{X}$ is the drainage velocity of the liquid slag;
g is the gravity acceleration;
ρ is the slag density;
$A_{plateau}$ is the area of the Plateau border through which the liquid slag is drained;
t is the time.

The area of the Plateau borders depends on the bubble size: the higher the bubble size is, the higher is the area featuring the Plateau borders (Figure 7). The relation (11) rules the drainage velocity of the liquid slag (Figure 8).
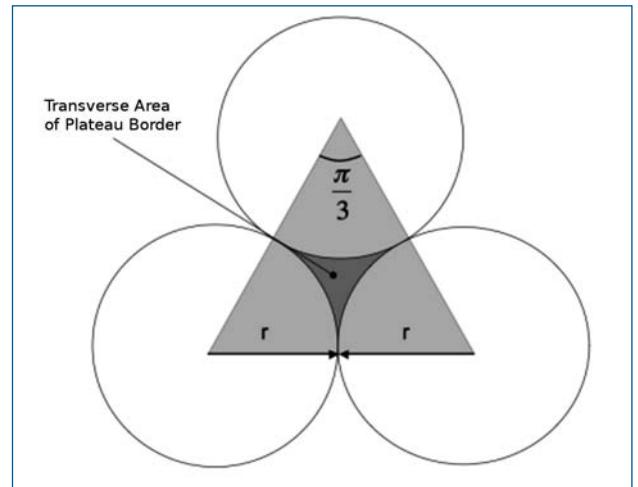
Fig. 7 - Area of the Plateau borders as a function of the bubble size [13].

Fig. 7 - Schema dell'area dei bordi di Plateau in funzione della dimensione delle bolle di gas [13].
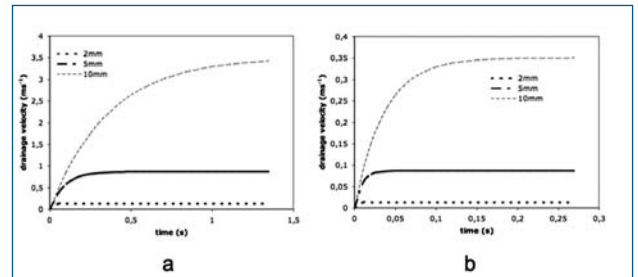
Fig. 8 - Trend of drainage velocity as a function of bubble radius and the viscosity (a) $43 \cdot 10^{-6}$ Pa·s (b) $500 \cdot 10^{-6}$ Pa·s [13].

Fig. 8 - Andamento della velocità di drenaggio della scoria liquida in funzione del raggio medio delle bolle e della viscosità (a) $43 \cdot 10^{-6}$ Pa·s (b) $500 \cdot 10^{-6}$ Pa·s [13].

EXPERIMENTAL TRIALS

The experimental observation have been performed on 2000 heats and the attention has been focused on the effect of $MgCO_3$ addition on the refractory wear and on the electric energy savings.
The charged scrap mix was featured by:
• 8% pig iron;
• 8% proler;
• 15% turning chips;
• 20% scrap from demolition;
• 50% thin plates.
The overall specific oxygen amount has been maintained constant at 30 Nm^3/t.
All the heats have been divided in four groups (each one

composed by 500 heats) featured by different addition of $MgCO_3$, CaO and anthracite injection (Table 1).

	MgCO$_3$ (kg/t)	CaO (kg/t)	Anthracite (kg/t)
Reference Case	–	40	15
Case 1	2	40	15
Case 2	5.5	35	13
Case 3	13	30	10

Table 1 - Investigated experimental conditions.

Tabella 1 - Condizioni sperimentali indagate.

The final main components of the EAF slag vary as a function of the performed addition (Table 2).

|	%FeO	%MgO	%CaO	%SiO$_2$	%MnO
Reference Case	38	3.8	25	15	6
Case 1	37	4.7	26	15	6
Case 2	40	7	23	12	6
Case 3	35	8	28	10	5

Table 2 - Main chemical species constituting the slag as a function of the different experimental conditions.

Tabella 2 - Specie chimiche principali costituenti la scorie nelle diverse condizioni sperimentali.

The specific refractory wear and the specific electric energy consumption have been monitored.
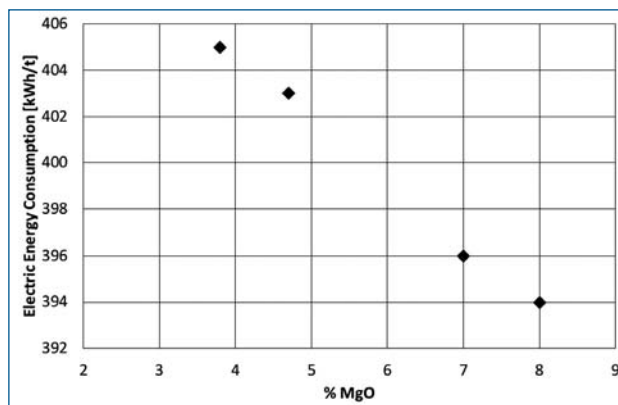
RESULTS
The average refractory wear and the specific electric energy consumption show a decreasing trend as the addition of $MgCO_3$ increases (Figure 9, Figure 10).
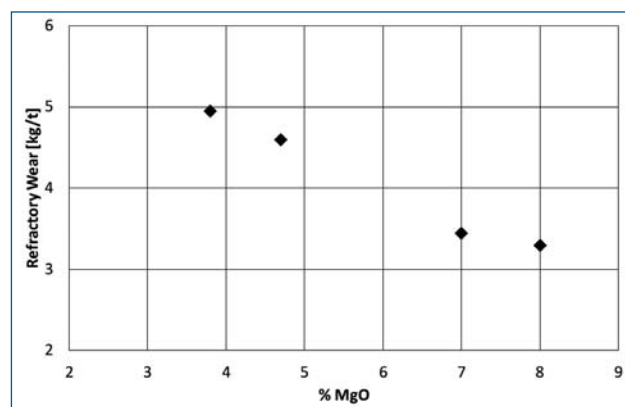
Fig. 9 - Specific refractory wear as a function of MgO weight concentration in slag.

Fig. 9 - Usura specifica dei refrattari in funzione della concentrazione in peso di MgO presente in scoria.

Fig. 10 - Specific electric energy consumption as a function of MgO weight concentration in slag.

Fig. 10 - Consumo specifico di energia elettrica in funzione della concentrazione in peso di MgO presente in scoria.

CONCLUSIONS

- The realization of stable foaming slag and inert for the refractory is a fundamental aim for the refractory protection;
- the use of $MgCO_3$ as an additive to the slag of the electric arc furnaces represents a very interesting opportunity, because it contributes to decrease the refractory wear and the specific electric energy consumption;
- the addition in $MgCO_3$ up to 13 kg/t can grant:
  - a 33% decrease of the refractory wear;
  - 4.8% saving of the electric specific energy, provided the same oxygen and methane specific flow rate. This advantage is associated to a decrease of the enthalpy absorption due to the formation of the gas bubbles;
  - decrease of the 18% of the charged lime (CaO);
  - decrease of the 33% of the injected graphite powder (usually constituted by anthracite).

REFERENCES

1] J. A. Duffy, M. D. Ingram, I. D. Sommerville. Acid-Base Properties of molten oxides and metallurgical slags. Journal of the Chemical Society, Faraday Transactions 1: Physical Chemistry in Condensed Phases 74 (1978) 1410–1419.

2] A. Lebouteiller, P. Courtine. Improvement of a bulk optical basicity table for oxidic systems. Journal of Solid State Chemistry 137 (1998) 94–103.

3] W. Nicodemi, C. Mapelli. Siderurgia. Associazione Italiana di Metallurgia, Milano (Italy), 2011, 292-294.

4] P. Pedersini, F. Maier, G. Alessandro, M. Maion, A. Romano. La produzione industriale di materiali refrattari, natura chimica, processi di trasformazione ed aspetti igienistici per la tutela della salute dei

lavoratori. Giornale Italiano di Medicina del Lavoro ed Ergonomia 34-3 (2012) 229-235.

5] G. Aliprandi, M. Cavallini. Breve storia dei refrattari. La Metallurgia Italiana 10 (2005) 63-73.

6] P.P. Budnikov. The technology of ceramics and refractories. Cambridge, The M.I.T. Press Ed. 1964.

7] J.H. Chester. Steelplant refractories. Sheffield, Percy Lund, Humphries & Co. Ltd. Ed. 1946.

8] A.A.V.V. Refractories Handbook, Chapter 3: Corrosion of Refractories, Marcel Dekker Inc., US, 2004, 39-49.

9] W.E. Lee, S. Zhang. Melt corrosion of oxide and oxide–carbon refractories. International Material Reviews 44-3 (1999) 77-104.

10] S. Sun, L. Zhang, S. Jahanshahi. From viscosity and surface tension to Marangoni flow in melts. Metallurgical and Materials transactions B 34B (2003) 517-532.

11] K. Mukai. Wetting and Marangoni effect in iron and steelmaking processes. ISIJ International 32-1 (1992) 19-25.

12] W. Nicodemi, C. Mapelli. Siderurgia. Associazione Italiana di Metallurgia, Milano (Italy), 2011, 169.

13] S. Barella, A. Gruttadauria, C. Mapelli, D. Mombelli. Critical evaluation of role of viscosity and gas flowrate on slag foaming. Ironmaking and Steelmaking 39-6 (2012) 463-469.

Prove sperimentali e aspetti teorici riguardanti schiumeggiamento della scoria, interazione scoria-refrattario e fattibilità di iniezione di magnesite cruda come agente schiumogeno e protettivo per il refrattario del forno elettrico ad arco

Parole chiave: Scoria - Refrattario - Schiumeggiamento - Iniezione di magnesite cruda

A seguito di un'approfondita disanima dell'interazione tra i refrattari del forno elettrico (Figura 1) e della loro interazione con le scorie (Figura 2, Figura 3, Figura 4), vengono indicati i fattori di influenza che provocano l'usura del refrattario e quelli che possono governare il fenomeno di schiumeggiamento necessario ad evitare la radiazione dell'arco elettrico sul refrattario stesso. Sulla base di tali indicazioni teoriche è stata realizzata una sperimentazione sistematica volta a chiarire i possibili vantaggi associati all'utilizzo di $MgCO_3$ quale agente schiumogeno e al fine di saturare in MgO la scoria, allo scopo di renderla compatibile con il refrattario. La scoria schiumosa si genera a seguito dell'interazione tra gocce di ossido di ferro, carbonio ed ossigeno iniettato (Figura 5), ma non è detto che la sola iniezione di carbonio sia un mezzo efficiente per generare le bolle; anzi vi sono evidenze sperimentali che mostrano come l'eccessivo utilizzo del polverino di carbone (in genere costituito da antracite) possa comportare inefficienze energetiche, che si sostanziano in aumento dell'energia elettrica specifica utilizzata (Figura 6). L'utilizzo di $MgCO_3$ garantisce invece lo sviluppo di fasi gassose nella scoria attraverso un inferiore assorbimento di calore. Inoltre, la saturazione della scoria in MgO comporta la precipitazione di fini particelle solide che aumentano la viscosità della scoria medesima, limitano il drenaggio della scoria liquida lungo i bordi di Plateau della scoria schiumosa (Figura 7) e quindi rendono più stabile l'emulsione schiumosa (Figura 8). I risultati ottenuti (Figura 9, Figura 10) dalle prove sperimentali (Tabella 1) mostrano i significativi vantaggi associati all'iniezione di $MgCO_3$, che indicano una diminuzione dell'usura del refrattario, una diminuzione dei consumi specifici di energia elettrica nonché un abbassamento nell'introduzione di calce e polverino di carbonio iniettato.